Hydrographic Changes in Nares Strait (Canadian Arctic Archipelago) in Recent Decades Based on δ^{18}O Profiles of Bivalve Shells

MARTA E. TORRES,[1,2] DANIELA ZIMA,[3] KELLY K. FALKNER,[1] ROBIE W. MACDONALD,[4] MARY O'BRIEN,[4] BERND R. SCHÖNE[5] and TIM SIFERD[6]

ABSTRACT. Nares Strait is one of three main passages of the Canadian Archipelago that channel relatively fresh seawater from the Arctic Ocean through Baffin Bay to the Labrador Sea. Oxygen isotopic profiles along the growth axis of bivalve shells, collected live over the 5–30 m depth range from the Greenland and Ellesmere Island sides of the strait, were used to reconstruct changes in the hydrography of the region over the past century. The variability in oxygen isotope ratios is mainly attributed to variations in salinity and suggests that the northern end of Nares Strait has been experiencing an increase in freshwater runoff since the mid 1980s. The recent changes are most pronounced at the northern end of the strait and diminish toward the south, a pattern consistent with proximity to the apparently freshening Arctic Ocean source in the north and mixing with Baffin Bay waters as the water progresses southward. This increasing freshwater signal may reflect changes in circulation and ice formation that favor an increased flow of relatively fresh waters from the Arctic Ocean into Nares Strait.

Key words: Arctic, Nares Strait, bivalves, time series, oxygen isotopes, salinity, fresh water

RÉSUMÉ. Le détroit de Nares est l'un des trois principaux passages de l'archipel canadien qui canalise de l'eau de mer relativement fraîche de l'océan Arctique jusqu'à la mer du Labrador en passant par la baie de Baffin. Les profils de la composition isotopique de l'oxygène le long de l'axe de développement des coquillages bivalves recueillis en vie à une profondeur variant entre 5 à 30 m des côtés du détroit à la hauteur du Groenland et de l'île d'Ellesmere ont servi à reconstruire les changements ayant caractérisé l'hydrographie de la région au cours du dernier siècle. La variabilité en matière de ratio d'isotope de l'oxygène est principalement attribuable aux variations de salinité, ce qui laisse entendre que l'extrémité nord du détroit de Nares connaît une augmentation de l'écoulement d'eau douce depuis le milieu des années 1980. Les changements récents sont plus prononcés à l'extrémité nord du détroit et diminuent en arrivant vers le sud, ce qui constitue une tendance conforme à la proximité de la source de l'océan Arctique en dessalure apparente dans le nord et qui se mélange avec les eaux de la baie de Baffin au fur et à mesure que l'eau progresse vers le sud. Cette augmentation de la présence d'eau douce peut être le reflet de changements en matière de circulation et de formation de la glace qui favorisent un écoulement accru d'eaux relativement douces en provenance de l'océan Arctique et se jettent dans le détroit de Nares.

Mots clés : Arctique, détroit de Nares, bivalves, série chronologique, isotope de l'oxygène, salinité, eau douce

Traduit pour la revue *Arctic* par Nicole Giguère.

INTRODUCTION

The Arctic Ocean plays a pivotal role in the global hydrologic cycle by returning waters evaporated and transported from the surface of the subtropical Atlantic Ocean to the North Pacific and circumpolar watersheds. The products of the freshwater input and mixing processes are exported back to the North Atlantic in the form of ice and freshened seawater through the western side of Fram Strait and the passages of the Canadian Arctic Archipelago (CAA) (Aagaard and Carmack, 1989; Melling, 2000; Melling et al., 2008). Model-based studies have shown that an increase in the freshwater export from the Arctic to the North Atlantic has the potential to hamper global ocean overturning circulation and consequently to affect the Northern Hemisphere climate (Renssen et al., 2001; Otterå et al., 2003; Saenko et al., 2003; Stouffer et al., 2006).

[1] College of Oceanic and Atmospheric Sciences, Oregon State University, 104 COAS Administration Building, Corvallis, Oregon 97331-5503, USA

[2] Corresponding author: mtorres@coas.oregonstate.edu

[3] AVI BioPharma, Inc., 4575 SW Research Way, Suite 200, Corvallis, Oregon 97333, USA

[4] Department of Fisheries and Oceans, Institute of Ocean Sciences, Sidney, British Columbia V8L 4B2, Canada

[5] Department of Applied and Analytical Paleontology, INCREMENTS Research Group, Institute of Geosciences, Earth System Science Research Center, University of Mainz, J.-J.-Becherweg 21, 55128 Mainz, Germany

[6] Freshwater Institute, 501 University Crescent, Winnipeg, Manitoba R3T 2N6, Canada

Over the past few decades, global and local environmental changes have influenced the distribution and storage of Arctic freshwater, including sea ice (e.g., Serreze et al., 2003; Walter et al., 2006; McPhee et al., 2009). A quantitative assessment of the variability and forcing of freshwater fluxes to and from the Arctic Ocean is essential in evaluating this region's sensitivity to natural and anthropogenic climate perturbations.

Bivalves are distributed throughout the CAA. The use of isotopic data from their shells is gaining significant attention as a valuable tool to generate a much-needed retrospective time series of hydrographic data (Khim et al., 2001, 2003; Müller-Lupp et al., 2003, 2004; Dettman et al., 2004; Simstich et al., 2005). These organisms accrete calcium carbonate at the ventral margin of their shells throughout the growing period, and this accretion is accentuated in the spring and summer. This process leads to the formation of annual growth increments throughout the bivalves' lives, which may extend from 10 to several hundred years (e.g., Rhoads and Lutz, 1980; Schöne et al., 2005a). The oxygen isotopic composition ($^{18}O/^{16}O$) of marine carbonate is controlled by the temperature and isotopic composition of the ambient water from which it precipitated. The isotope data are commonly expressed in the conventional delta (δ) notation,

$$\delta^{18}O = 1000 * (^{18}O/^{16}O_{sample} - {}^{18}O/^{16}O_{reference})/ {}^{18}O/^{16}O_{reference}, (1)$$

where the isotope ratios of the carbonate ($\delta^{18}O_{carb}$) are reported relative to the international Vienna Pee Dee Belemnite (V-PDB) standard. The oxygen isotopic composition of the ambient water ($\delta^{18}O_{water}$) is reported relative to V-SMOW (Vienna Standard Mean Ocean Water). The $\delta^{18}O_{water}$ in turn is influenced primarily by the amount of freshwater from runoff, direct precipitation, and sea-ice formation, and to a lesser extent, by glacial melt (Alkire, 2010). Thus, by establishing oxygen isotopic profiles of the carbonate shells along the axis of maximum growth, it is possible to obtain hydrographic time-series information on the bivalve's habitat. Here we combine hydrographic data with isotopic analyses of bivalves recovered live from Nares Strait to document these relationships. The observed shell records suggest a freshening as early as the mid 1980s, a timing that is in agreement with limited tracer hydrographic information and model-based considerations, as discussed below.

STUDY AREA

The upper Arctic Ocean stores nearly 100 000 km³ of freshwater (including sea ice). The principal inputs of freshwater include 3200 km³/yr from large rivers in Russia and Canada, about 2500 km³/yr freshwater equivalent flow of Pacific seawater entering through Bering Strait, and 2000 km³/yr of direct precipitation minus evaporation (Aagaard and Carmack, 1989; Bauch et al., 1995; Macdonald et al.,

2002; Woodgate and Aagaard, 2005; Serreze et al., 2006, 2008). As they are isotopically indistinguishable, we refer to the combined run-off and direct precipitation to the Arctic as meteoric.

The freshwater inventory of the Arctic Ocean provides the potential for the system to export large pulses of freshwater to the North Atlantic. Changes in the Arctic freshwater budget and circulation appear to be associated with changing atmospheric pressure patterns (Dickson et al., 2000; Serreze et al., 2000; Bauch et al., 2009) and global warming trends (Peterson et al., 2002). If these changes result in enough freshwater spreading to the deep convection regions in the Labrador Sea, they may hinder convection or even prevent waters from attaining sufficient density to sink and ventilate the upper deep ocean.

Nares Strait is one of three main passages of the CAA that channel relatively fresh seawater from the Arctic Ocean through Baffin Bay to the Labrador Sea (Fig. 1). The head of Nares Strait is situated just downstream from the confluence of the Transpolar Drift and the Beaufort Gyre, where Atlantic and Pacific water masses meet (Karcher and Oberhuber, 2002; Steele et al., 2004). Seasonal and interannual variability in Arctic Ocean circulation as expressed in the upper 220 m (the approximate sill depth in Kane Basin) will be manifest in Nares Strait before propagating into Baffin Bay, across Davis Strait, and into the Labrador Sea (Steele et al., 1996).

Salinity – $\delta^{18}O$ Relationships

Chemical characterization of Arctic waters has been a subject of several investigations aimed at establishing the various water types of the central Arctic Ocean and passages of the CAA. This chemical analysis can be used to derive insights into ocean circulation and the region's hydrographic response to climate change (e.g., Alkire et al., 2007; Yamamoto-Kawai et al., 2005, 2008; Guay et al., 2009). Among the various available geochemical tracers, salinity – $\delta^{18}O$ relationships have been used since the 1980s (e.g., Östlund and Hut, 1984; Tan and Strain, 1980, 1996; Strain and Tan, 1993; Macdonald et al., 1995) as a means of quantifying the seasonal icemelt and meteoric water contributions to the freshwater budget. Alkire (2010) recently constrained the net contributions of these two components by applying conservation equations to an extensive hydrographic data set collected from our study area in 1997 and 2003.

MATERIALS AND METHODS

Sampling Sites

Bivalves were collected at five locations on the Greenland and Ellesmere Island sides of Nares Strait during Healy cruise 031 from 2 to 14 August 2003 (Fig. 1B). The sampling sites, identified during a helicopter reconnaissance survey, were selected to optimize exposure to the
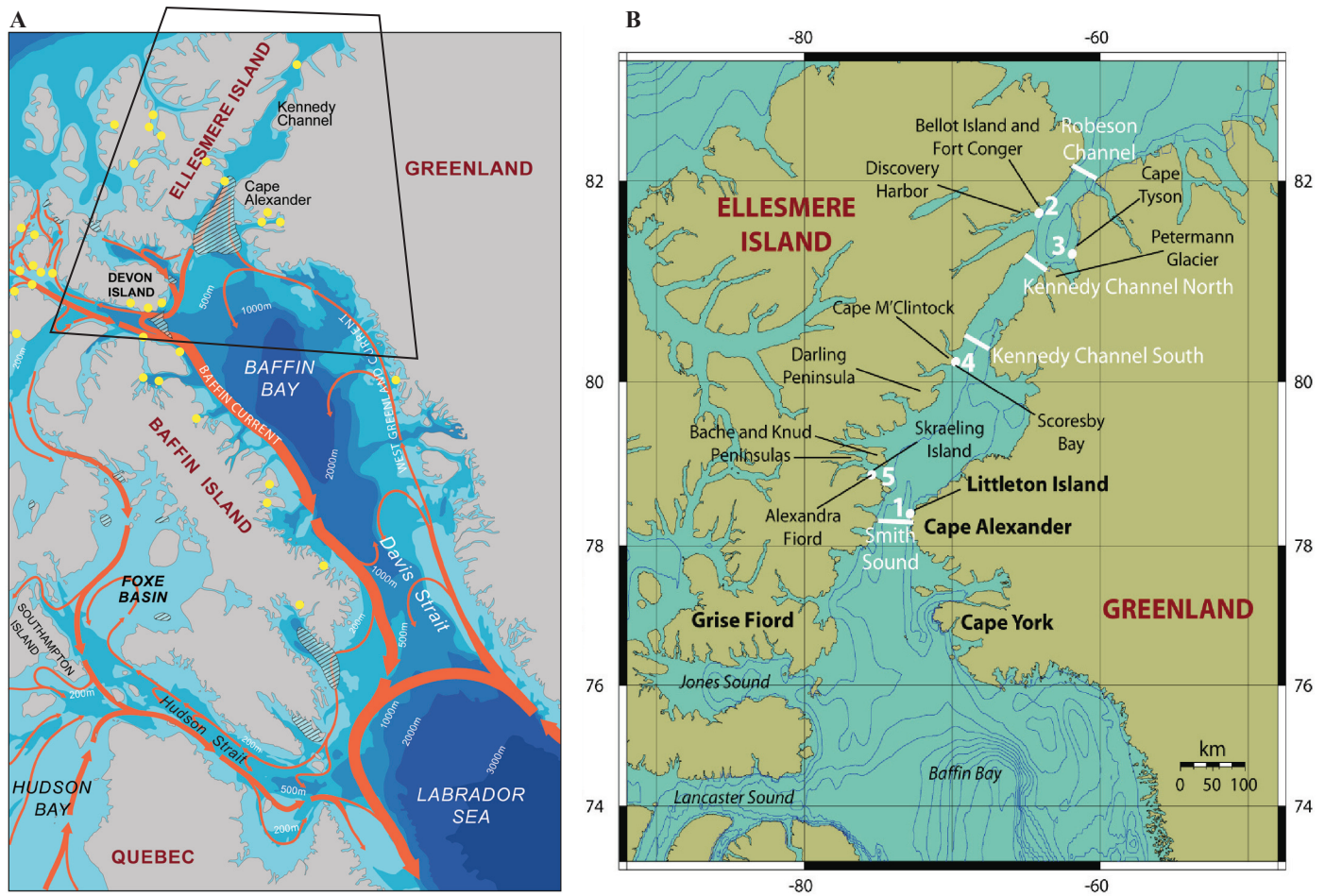
FIG. 1. Study area modified from http://www.ibcao.org. A. Surface circulation patterns south of the Canadian Arctic Archipelago and Baffin Bay. The red arrows indicate the direction of current flows, and the width indicates the relative magnitude of water that is transported with the currents (from Falkner et al., 2006). Yellow dots indicate regions where previous bivalve studies have been conducted as referenced in Zima (2007). Box denotes the location of Nares Strait. B. View of the Nares Strait general study area between northern Greenland and Canada. Solid white lines represent transects for water sampling at Smith Sound, Kennedy Channel South, Kennedy Channel North, and Robeson Channel used by Alkire (2010) to constrain salinity-δ^{18}O relationships for this area. Numbers in white represent stations of bivalve collection for this study, listed in Table 1.

main water flow in the strait and to ascertain the absence of nearby freshwater streams. A relatively steeply sloping bottom was sought to permit safe sampling by divers. Sampling sites were surveyed with a submersible color camera to identify the siphons and closed shells of living bivalves. Soft sediment mixtures of sand, gravel, and clay compose their benthic habitat.

Station 1 was located on the western side of Littleton Island in a small, protected channel. The site was approximately 6 m deep, with abundant kelp, brittle stars, and prevalent bivalve siphons. At Station 2, bivalves were collected on the east side of Bellot Island, over a relatively gently sloping bottom that was muddy and free of macroalgae. Station 3 was located on the eastern side of Offley Island. The area bordering Station 4 in Scoresby Bay consisted of exposed coastline, with abundant grounded ice and regions of scour in the shallows. Western Scoresby Bay was dominated by large inflowing rivers, so sampling was sited at the northeastern mouth of the bay. Station 5 was located in Alexandra Fiord, just southwest of Cairn Island. Station coordinates and specimens recovered are listed in Table 1.

A total of 198 bivalves of 8 different species were collected over the depth range of 6 to 30 m. Total length, width, and wet weight (shell + body) were measured onboard after collection, and are reported elsewhere (Zima, 2007).

Water and Bivalve Analyses

Seawater samples for salinity and oxygen isotope measurements were collected at each site through deployment of a 1.7 L Niskin bottle at the depths of bivalve collection (Table 2). A full hydrographic data set for this region, obtained as part of the Canadian Archipelago Throughflow Study (CATS), is archived at the CLIVAR & Carbon Hydrographic Data Office (CCHDO) and is available online at http://www. udel.edu/CATS/data/CTD2003/. Oxygen isotope data from these sections have been reported in Alkire (2010).

Salinities were measured on board in a temperature-controlled room using an Autosal by Guildline, Model 8400B (#65-715), with a precision of 0.002 PSU (Practical Salinity Units). The oxygen isotopic composition of the water ($\delta^{18}O_{water}$) was analyzed at Oregon State University by the

TABLE 1. Summary of sites on both sides of Nares Strait from which bivalves were collected during August 2003. Site locations are shown in Figure 1.

Collection date in 2003	Site name (number)	Latitude N	Longitude W	Depth range (m)	Species (number of live specimens)[1]
August 2	Littleton Island (Station 1)	78˚ 22.20′	72˚ 51.0′	6	HA (1); SG (1)
August 7	Bellot Island (Station 2)	81˚ 42.81′	64˚ 55.0′	13 – 27	AB (28); HA (15); MT (4); NB (1); PA (13); SG (3)
August 10	Offley Island (Station 3)	81˚ 17.91′	61˚ 43.93′	10 – 20	HA (1)
August 12	Scoresby Bay (Station 4)	79˚ 55.80′	71˚ 7.0′	10 – 20	AB (11); HA (3); MT (6); NB (1); NP (1); SG (3)
August 14	Alexandra Fiord (Station 5)	78˚ 54.35′	75˚ 47.16′	6 – 22	AB (84); HA (2); MC (6); MT (5); NB (2); NP (2); SG (5)

[1] HA = *Hiatella arctica*, SG = *Serripes groenlandicus*, AB = *Astarte borealis*, MT = *Mya truncata,* NB = *Nucula bellotti*, PA = *Portlandia arctica*, and NP = *Nuculana pernula*.

TABLE 2. Salinity and oxygen isotopic composition of the water at the bivalve collection sites.

Bivalve collection site	Depth (m)	Salinity	$\delta^{18}O_{water}$ (‰V-SMOW)
Station 1, Littleton Island	1	31.757	-1.88
	5	31.757	-1.87
	10	31.804	-1.78
	20	31.933	-1.73
Station 2, Bellot Island	1	31.254	-2.67
	5	31.369	-2.68
	10	31.378	-2.67
	20	31.448	-2.61
	30	31.573	-2.58
Station 3, Offley Island	1	30.019	-3.45
	8	30.096	-3.37
	17	30.484	-3.17
Station 4, Scoresby Bay	1	30.823	-2.76
	5	31.464	-2.38
	10	31.631	-2.27
	20	31.894	-2.22
Station 5, Alexandra Fiord	1	31.256	-2.23
	5	31.260	-2.20
	10	31.766	-2.02
	18	32.122	-1.85

CO_2 equilibration method, using a Finnigan Mat 251 mass spectrometer. Results are reported relative to V-SMOW, and 1-sigma precision is estimated to be ± 0.05‰.

Bivalve shells were ultrasonically rinsed in water-free ethyl alcohol and coated with J-B® KWIK WeldTM quick-drying metal epoxy to form a protective coating during cutting, grinding, and polishing. Mirror-image sections (1 – 3 mm thick) for sclerochronological and isotope analysis were cut from the shells perpendicular to the growth axis, using a diamond band saw. Details of the procedures used are given in Schöne et al. (2004). Growth layers were determined by microscopic examination of shells stained with Mutvei's solution (500 mL 1% acetic acid, 500 mL 25% glutaraldehyde, and 5 g of alcian blue powder), following the techniques of Schöne et al. (2005b). Treated samples were then viewed under a Leica DMLP reflected light binocular microscope with 16× or 25× magnification and equipped with a Nikon Coolpix 995 camera.

Immersion in Mutvei's solution produces a crisp, three-dimensional relief of etch-resistant ridges (growth lines) and etched depressions (growth increments) (Fig. 2). The growth lines are stained a deeper blue than the growth increments because more polysaccharides and soluble organics are deposited or accumulated in the hard parts

during periods of reduced $CaCO_3$ precipitation and skeletal growth (e.g., Schöne et al., 2004). The ontogenetic age for each individual is assigned by counting these banded pairs of annual growth increments.

The unstained shell segments directly opposing the stained cross-section were sampled using a 1 mm diameter cylindrical diamond drill bit (Brasseler USA) under a stereo-microscope (10× to 20× magnification). Each drilling yielded approximately 50 μg or less of carbonate powder, which was collected from the outer shell layer along the growth axis in roughly annual increments. The oxygen isotope values in the carbonate ($\delta^{18}O_{carb}$) were measured at Oregon State University using a Finnigan/MAT 252 stable isotope mass spectrometer equipped with a dual-inlet and Kiel-III carbonate preparation device, with a precision of ± 0.06‰. Isotope values are reported relative to the V-PDB scale.

RESULTS

Hydrographic Data

The hydrographic data for the bivalve collection sites are given in Table 2. Data from bivalve sites are in accord with the salinity – $\delta^{18}O_{water}$ relationship for the upper waters of the Nares Strait region reported by Alkire (2010). The variation of $\delta^{18}O_{water}$ as a function of salinity in Nares Strait, displayed in Figure 3, shows a reasonable fit to a line defined by:

$$\delta^{18}O_{water} = 0.69 \bullet Salinity - 24.2‰ \qquad (2)$$

Within uncertainties, this line is consistent with the mixing of Atlantic and Pacific source waters with those of high-latitude meteoric inputs, and it includes a component of a net ice formation signal from the Arctic interior (Münchow et al., 2006; Alkire, 2010). Taking into account error in both the salinity and the $\delta^{18}O_{water}$ measurements, this relationship implies a freshwater $\delta^{18}O_{water}$ end member of -24.2‰ (± 1.1 at the 95% confidence interval, Fig. 3). The Arctic Ocean that supplies Nares Strait carries a meteoric water end-member signal of -18.8 ± 2‰, which has been calculated from a flow-weighted average of river runoff (Cooper et al., 2008). The lower value reported here (-24.2‰) reflects an additional contribution by halocline water that is brine-enriched during sea-ice formation in the Arctic.
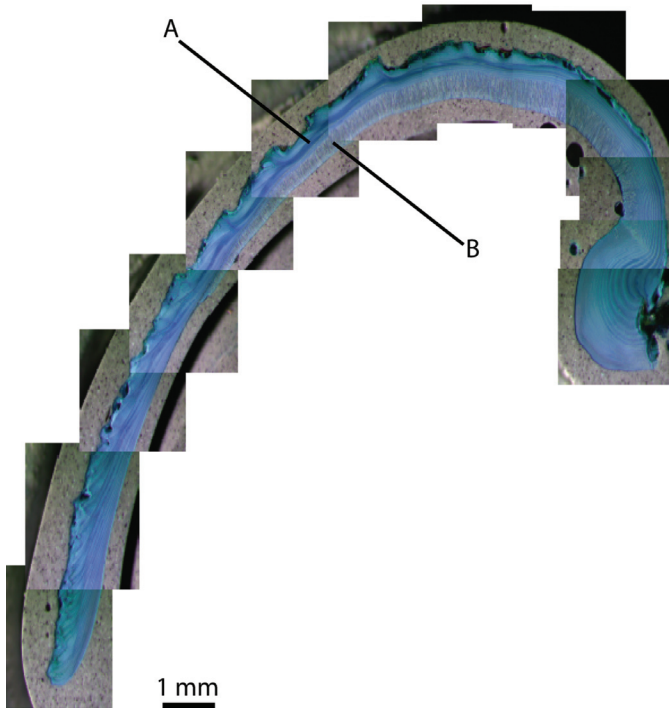
FIG. 2. Composite cross-section of *Hiatella arctica* stained with Mutvei's solution, where (A) represents the outer shell layer and (B) represents the inner shell layer. Darker stained portions of the shells indicate winter growth, while lighter-blue stained portions represent summer growth.

FIG. 3. Relationship between salinity and $\delta^{18}O_{water}$ for the Nares Strait region (line intercept = -24.2 ± 1.1‰ and slope = 0.69 ± 0.03, at the 95% confidence interval; n = 170; r^2 = 0.95). The equation describes the extrapolation of the salinity-$\delta^{18}O_{water}$ relationship for Nares Strait to the implied freshwater (S = 0) end-member $\delta^{18}O_{water}$ value (-24.2 ± 1.1‰). The Pacific end member for salinity 33.1 is -1.1 ± 0.1‰ (Macdonald et al., 2002) and the Atlantic end member for salinity 34.9 is about 0.3‰ (Bauch et al., 1995). The low freshwater end-member value reflects a contribution of halocline waters imported from the Arctic (Alkire, 2010).

This brine-enriched water is retained as these waters flow southward (Alkire, 2010). Although identifying the various components that define the $\delta^{18}O_{water}$ − salinity relationships is critical to accurately estimating freshwater contributions (Alkire, 2010), for a first-order interpretation of our results we will take the observed relationship at face value, assume it is relatively constant in time, and assign an "apparent" freshwater end member of -24.2 ± 1.1‰. It is important to recognize that either more meteoric input or less brine from sea ice formation (or both) can lead to "freshening."

Bivalve Data

The bivalve species composition varied from station to station (Zima, 2007), but in general, specimens of *Nucula bellotti*, *Nuculana pernula*, *Mya truncata*, *Serripes groenlandicus*, and *Macoma calcarea* were most prevalent in shallower waters (to approximately 20 m). These individuals were also predominantly small and young (10 to 20 years old or less). Older bivalves were represented by the species *Astarte borealis* and *Hiatella arctica* and were found to be abundant at three of the five stations (Table 1). *A. borealis* was found at all depths at these stations and spanned the largest age range, from about 20 to 150 years (± 10 years). All the *H. arctica* for age analysis were collected live at Bellot Island over nearly the entire depth range up to approximately 30 m, and ranged in age from 5 to 50 years (± 2 years). The ages obtained in this study for *M. truncata* (14 years), *S. groenlandicus* (8 years), and *H. arctica* (5 to
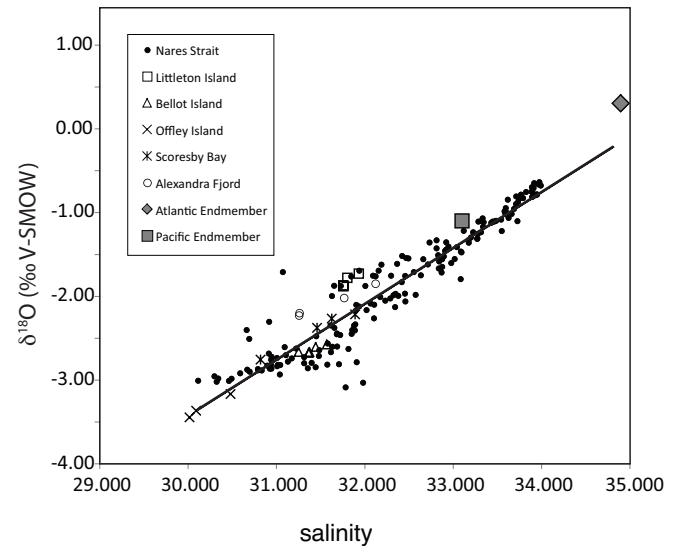
22 years), shown in Table 3, agree well with the typical life spans for these individuals reported by other investigators (Sejr et al., 2002; Amaro et al., 2003; Kilada et al., 2007). The estimated ages for *A. borealis* (20 to 150 years) are significantly higher than the maximum age of 8 years for specimens with similar shell lengths reported by Selin (2007). However, data from Müller-Lupp and Bauch (2005) reflect ages greater than 15 years for *A. borealis* specimens from the Laptev Sea, and previous analyses of *A. borealis* shells from the North Sea revealed ages of ca. 50 years (Degen, 2005). Errors associated with the counting of growth rings in specimens of *H. arctica* (± 2 years) are lower than those associated with *A. borealis* (± 10 years) because ontogenetic effects (slower metabolism and generation of new shell material with age) cause the growth rings of *A. borealis* to crowd together. Thus, discerning annual growth increments for *A. borealis* individuals becomes more of a challenge as they age; nonetheless, even taking into account the errors in our measurement (± 10 years), the *A. borealis* specimens studied here reach ages significantly greater than those previously reported for this species.

The age and measured oxygen isotopic composition in the youngest sections of all specimens analyzed are listed in Table 3. Also listed are ontogenetic age and isotopic data for entire shells of *A. borealis* and *H. arctica* collected from stations 2, 4, and 5. The isotope distribution as a function of age for whole shells of *A. borealis* specimens is shown in Figure 4. The composite data set shows a relatively stable isotope signal except for the specimens collected in the northernmost region of Nares Strait (Bellot Island, Station 2), where a striking trend towards lighter values is apparent

TABLE 3. Measured $\delta^{18}O_{carb}$ values in the youngest sections of bivalves of all studied species, as well as whole shells of *H. arctica* and *A. borealis* from Bellot Island (Station 2), Scoresby Bay (Station 4), and Alexandra Fiord (Station 5). Continued on p. 7.

Stn	ID	Species (ontogenetic age in years)	Depth (m)	Annual increments sampled (yrs)	$\delta^{18}O_{carb}$ (‰VPDB)	Stn	ID	Species (ontogenetic age in years)	Depth (m)	Annual increments sampled (yrs)	$\delta^{18}O_{carb}$ (‰VPDB)
2	4	NB (6)	13.4–14.3	1	-1.74	2	33	AB (150)	18.6	1–5	-1.94
2	5	PA (30)	13.4–14.3	1	2.42					6–17	-0.98
2	17	HA (9)	13.4–14.3	1	0.10					18–29	-0.91
				2	0.00					30–41	0.26
				3	0.19					42–51	1.06
				4	1.21					52–56	1.06
				5	-0.31					57–66	1.35
				6	1.73					67–76	1.49
				7	1.46					77–86	1.61
				8–9	1.75					87–96	1.41
2	18	HA (9)	13.4–14.3	1	1.40					97–116	1.74
				2	0.88					117–126	1.36
				3	1.88					127–131	0.94
				4	1.28					132–150	0.77
				5	1.44	2	35	AB (60)	18.6	1	1.23
				6	2.54					2	1.65
				7	1.72					3	1.58
				8	2.20					4–6	1.51
				9	0.07					7–9	1.93
2	22	AB (125)	13.4–14.3	1–6	2.09					10–12	2.11
				7–9	1.93					13–15	2.15
				10–12	2.09					16–20	2.15
				13–15	2.30					21–25	2.17
				16–19	2.33					26–30	1.77
				20–25	2.22					31–36	2.07
				26–28	2.40					37–39	1.64
				29–33	2.22					40–45	1.76
				34–40	2.03					36–51	1.87
				41–45	2.19					52–58	2.06
				46–51	2.35					59–60	1.54
				52–62	2.30	2	43	AB (45)	18.6	1	-0.02
				63–65	2.30	2	46	HA (19)	21.6–23.2	1	0.32
				66–70	2.05					2	0.78
				71–90	1.13					3	-0.11
				91–100	1.27					4	1.43
				101–105	1.55					5	0.71
				106–110	2.05					6	1.36
				111–115	1.64					7	0.83
				116–120	2.18					8	-0.86
				121–125	1.44					9	0.10
2	24	AB (20)	13.4–14.3	1	-4.87					10	0.84
				2	-1.85					11	0.52
				3	-0.77					12	0.08
				4–5	0.22					13	1.10
				6–7	1.21					14	1.19
				8	1.14					15	1.31
				9	-0.48					16	1.07
				10	2.12					17	1.11
				11	-0.50					18	-0.18
				12	0.95					19	-1.02
				13	1.83					15	1.31
				14	1.52					16	1.07
				15	1.93					17	1.11
				16–18	1.72						
				19–20	1.10						
2	29	PA (55)	15.8	1	-1.05						
2	31	AB (95)	15.8	1	1.76						

in the most recent years of growth. The relatively stable signal observed in most samples indicates that there is no apparent ontogenetic effect on the isotopic composition of the shell, which is consistent with isotope records reported in the literature for *A. borealis* and *S. groenlandicus* from various Arctic regions (e.g., Israelson et al., 1994; Khim et al., 2003; Müller-Lupp et al., 2003).

DISCUSSION

Calibration of the Expected $\delta^{18}O$ Equilibrium

A few X-ray diffraction analyses of the carbonate material showed it to consist predominantly of aragonite, in agreement with literature data documenting aragonite shell

TABLE 3. Measured $\delta^{18}O_{carb}$ values in the youngest sections of bivalves of all studied species, as well as whole shells of *H. arctica* and *A. borealis* from Bellot Island (Station 2), Scoresby Bay (Station 4), and Alexandra Fiord (Station 5) – *continued*:

Stn	ID	Species (ontogenetic age in years)	Depth (m)	Annual increments sampled (yrs)	$\delta^{18}O_{carb}$ (‰VPDB)
2	47	HA (22)	21.6–23.2	1	-1.28
				2	-0.35
				3	-1.71
				4	-0.30
				5	-0.85
				6	-0.26
				7	-1.62
				8	-0.68
				9	-0.33
				10	-0.73
				11–12	-0.09
				13	1.30
				14	1.34
				15	-0.17
				16	0.04
				17–18	1.71
				19	1.69
				20–22	1.84
2	48	HA (5)	21.6–23.2	1	-0.23
				2–3	0.99
				4–5	1.04
2	52	AB (90)	21.5–23.0	1	0.97
2	54	AB (54)	21.5–23.0	1	1.08
2	65	AB (35)	27.3	1	-0.23
2	66	AB (60)	27.3	1	0.62
3	67	HA (20)	19.1	1	1.91
4	73	AB (80)	12.8	1	1.93
				2	1.97
				3	2.07
				4	2.38
				5	2.04
				6–8	2.22
				9–11	1.79
				12–14	1.83
				15–19	2.00
				20–25	2.06
				26–31	1.44
				32–35	1.61
				36–41	2.13
				42–45	1.55
				46–50	1.91
				51–56	2.13
				57–61	2.13
				62–66	2.18
				67–71	1.87
				72–80	1.73
4	74	AB (40)	12.8	1	1.59
				2	2.30
				3	1.48
				4	1.88
				5–6	1.72
				7–8	1.74
				9–10	2.01
				11–15	2.09
				16–20	2.35
				21–30	2.05
				31–40	1.81

Stn	ID	Species (ontogenetic age in years)	Depth (m)	Annual increments sampled (yrs)	$\delta^{18}O_{carb}$ (‰VPDB)
4	75	AB (80)	12.8	1–12	1.96
				13–17	1.89
				18–21	2.05
				22–25	2.36
				26–29	2.32
				30–35	2.13
				36–40	1.92
				41–51	2.40
				52–61	1.51
				62–70	1.57
				71–75	1.79
				76–80	2.30
4	68	SG (8)	9.7	1	0.37
4	71	MT (20)	12.8	1	1.98
4	77	NP (25)	16.7	1	1.53
4	78	AB (40)	16.7	1	1.62
4	81	NB (26)	16.7	1	1.63
4	87	AB (80)	20.1	1	-0.10
				2–6	1.10
				7–11	1.46
				12–16	1.53
				17–26	1.75
				27–36	1.47
				37–46	1.02
				47–56	1.08
				57–76	1.23
				77–80	1.12
5	94	MT (14)	6.7	1	2.03
5	95	AB (32)	6.7	1	1.87
5	102	MC (23)	18.9–19.8	1	0.95
5	105	NB (60)	18.9–19.8	1	3.22
5	106	NP (13)	18.9–19.8	1	2.17
5	126	AB (80)	18.9–19.8	1–10	2.24
				11–20	2.58
				21–30	2.41
				31–40	2.62
				41–50	2.26
				51–60	1.98
				61–70	1.84
				71–74	2.16
				75–80	2.41
5	136	AB (30)	18.9–19.8	1	2.14
5	142	AB (80)	18.9–19.8	1–10	1.78
				11–20	2.28
				21–44	2.12
				45–55	2.90
				56–65	1.83
				66–75	1.81
				76–80	1.61
5	146	AB (150)	18.9–19.8	1	2.12
5	157	MC (10)	22.1	1	2.14
5	182	AB (30)	22.1	1	1.80
5	187	AB (90)	22.1	1–12	1.89
				13–32	2.19
				33–52	2.15
				53–67	2.13
				68–86	2.00
				87–90	1.54
5	192	AB (50)	22.1	1	2.29
5	193	AB (80)	22.1	1	2.42

composition for all the species studied here (e.g., Wassenaar et al., 1988; Khim, 2002; Khim et al., 2003; Müller-Lupp et al., 2003; Simstich et al., 2005). The expected isotopic composition of the aragonite ($\delta^{18}O_{carb}$) can be predicted from thermodynamic equilibrium with the isotopic composition of the ambient water ($\delta^{18}O_{water}$) at a given temperature (T), according to the following empirical equation (modified from Böhm, 2000):
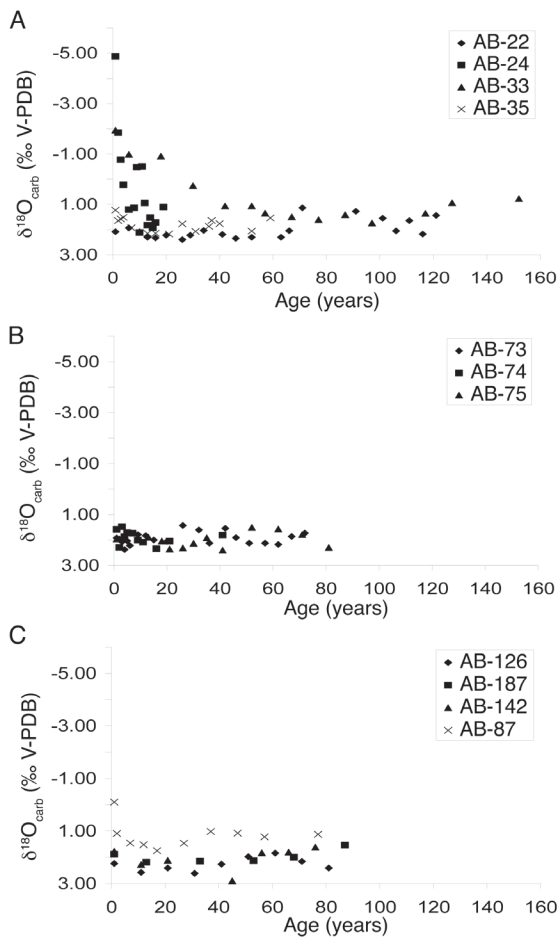
FIG. 4. Oxygen isotope composition versus age for specimens of *A. borealis* (AB) collected from (A) the northernmost region of Nares Strait at Station 2, (B) midway through at Station 4, and (C) the southernmost region at Station 5. Sample ID numbers are those given in Table 3.

$$\delta^{18}O_{carb} = 4.52 - 0.23T + \delta^{18}O_{water} \qquad (3)$$

Although this relationship was originally derived for sponges, it has been successfully applied to hydrographic reconstructions for Arctic regions using data obtained from shells of *A. borealis*, *S. groenlandicus*, and *Macoma calcarea* from Holocene to modern times (Müller-Lupp et al., 2004; Simstich et al., 2005). On the basis of the strong correlation between the $\delta^{18}O_{water}$ and salinity shown in Figure 3, we rewrite the above equation as:

$$\delta^{18}O_{carb} = (4.52 - 0.23T) + (0.69\text{Salinity} - 24.2), \qquad (4)$$

which allows us to evaluate variation in the oxygen isotopic record of the shell as a function of temperature and salinity.

Time series data collected continuously from 2003 to 2006 indicate that the maximum temperature range observed in our study area is ~8° (-2°C to 6°C; Rabe et al., 2010). We thus selected temperatures at 2°C intervals over the whole range observed in this region and calculated the expected shell isotopic values for each temperature value, which are plotted as discrete lines on Figure 5. This figure also shows the oxygen isotopic composition of a specimen
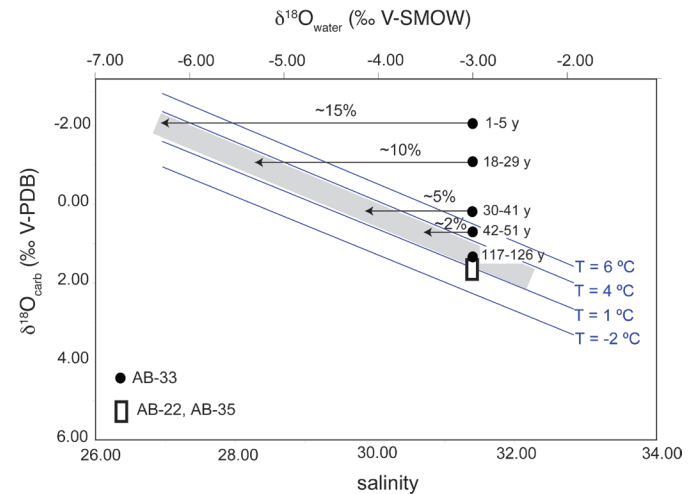
FIG. 5. Expected isotopic composition of the aragonitic shells (solid lines) precipitated in equilibrium with the oxygen isotopic composition of the ambient water (which is here assumed to be a salinity proxy, using the transfer function shown in equation 2), at discrete temperatures (which encompass the maximum temperature ranges observed at the region from 2003 to 2006 by Rabe et al., 2010). Measured $\delta^{18}O$ shell composition of an *A. borealis* shell (AB-33, black dots) at discrete ontogenetic ages, expressed as number of years before collection date, shows significant deviations from the expected values, which become larger in the more recent years. Other specimens of *A. borealis* (AB-22 and AB-35) have isotopic records that are in apparent equilibrium with the ambient salinity and temperature (shown by rectangle).

of *A. borealis* (AB-33, black dots) at different ontogenetic ages (denoted as time slices in years). The spread in isotopic values for this shell contrasts with the results from other specimens (AB-22 and AB-35, shown by a rectangle), which have an isotopic record that is in apparent equilibrium with the ambient salinity (31.4) and temperature of calcification (~1 ± 0.5°C). In this exercise, the records from AB-22 and AB-35 (and those from samples shown in Fig. 4B and C, but not included in Fig. 5) show that the isotopic composition of the shells can indeed be used in combination with equation (4) to reconstruct the hydrographic conditions of the bivalve's habitat. In light of this, it becomes apparent that the record of AB-33 reflects either unrealistically warm water or a dilution of the ambient water with fresher, isotopically light waters. If we assume that the ambient waters where this bivalve grew have not been warmer than 4°C, then the isotopic data reflect a freshening effect of up to 15%. Similar combinations of potential temperature/salinity conditions can be deduced from Figure 5, but in all cases the isotopic record shows that AB-33 experienced progressively fresher and perhaps warmer waters during the past 50 years.

To further evaluate the isotopic variations in our full data set, we compared the isotopic composition of the carbonate accreted during the most recent years of growth of 42 bivalves to expected values at equilibrium temperatures ranging from -2°C to 6°C (Fig. 6). In the most recent years, many of the shells collected from Bellot Island (Station 2) and some specimens from Scoresby Bay (Station 4) show isotopic values that are significantly lighter than those expected from the maximum temperature values. The
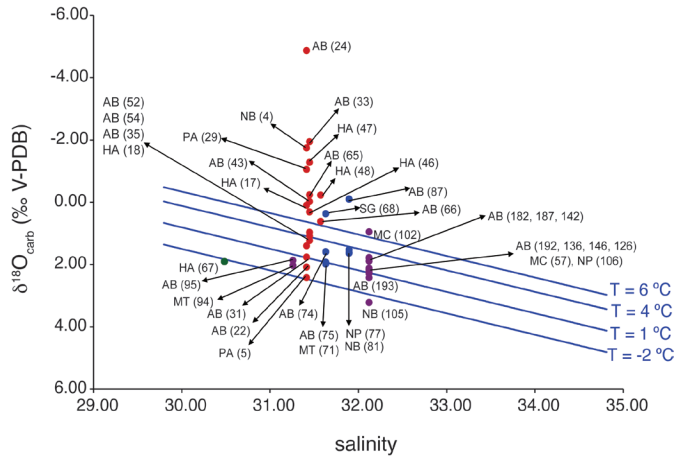
FIG. 6. Measured δ^{18}O shell composition in the youngest sections (< 3 years) of bivalve shells collected from all stations in Nares Strait as a function of temperature, using hydrographic data listed in Table 2 (for the depth of bivalve collection) and isotopic values listed in Table 3 (for the most recent year of growth). The expected isotopic composition of the aragonitic shells precipitated in equilibrium at discrete temperatures is shown by the long parallel lines. Red circles represent samples from Bellot Island, purple circles designate Alexandra Fiord, green circles represent Offley Island, and blue circles represent Scoresby Bay. Letters represent the bivalve species as indicated in Table 1, and numbers correspond to the specimen identification numbers listed in Table 3.

deviations from expected values are apparent in all species analyzed and are independent of sample collection depth and specimen age. The observed δ^{18}O$_{shell}$ data reach values as negative as -4.87‰, with several samples showing values more negative than -1.00‰. If we assume that this signal derives entirely from dilution with meteoric waters, it implies salinities ranging from 23 to 26, assuming an ambient temperature of 1°C to 2°C (Eq. 4). Of course, this example represents an extreme set of assumptions. The reality likely involves a combination of meteoric dilution and possibly reduced brine production or a temperature increase, or both. Nonetheless, a freshening effect is required to account at least partially for the observed isotopic variability. Anomalously light δ^{18}O$_{shell}$ values are most pronounced in specimens collected from Bellot Island (Station 2) at the northern end of Nares Strait, and the magnitude of the deviations from the expected range decreases from north to south.

We also examined time slices of shells corresponding to 10 (± 5), 20 (± 10), 30 (± 10), and 40 (± 10) years in specimens of *A. borealis* and *H. arctica* collected from Bellot Island (Station 2), Offley Island (Station 3), and Alexandra Fiord (Station 5), which represented stations at the inlet, midpoint, and outlet of Nares Strait, respectively (Fig. 7). Measured isotopic records in *A. borealis* and *H. arctica* corresponding to the 10 and 20 year shell sections from Bellot Island (Station 2) were significantly lighter than the expected values, even if we assume a high temperature of 6°C. The shell sections accreted 30 to 40 years ago show isotopic values that fall within the expected range given the salinities and temperatures measured in Nares Strait.

These data are compiled in Figure 8, which shows that the largest deviations from expected oxygen isotopic values at the average and maximum temperatures recorded in Nares Strait (1°C and 6°C) occur most frequently in the youngest shell sections (< 3 year time slice), and decrease progressively in frequency and magnitude to the 30 and 40 year time slices. These results reveal that the measured δ^{18}O values in the bivalve shells have been getting significantly lighter in the recent past compared to 30, 40, and even 20 years ago.

Bivalves as Hydrographic Indicators

A one-time acoustic Doppler survey along with hydrographic sections (Münchow et al., 2006) and preliminary results from a moored array of the CATS program (Rabe et al., 2010) estimate that 800 ± 400 km³/yr of freshwater pass through Nares Strait, an amount that constitutes about one-fourth of the estimated flux from the Arctic. While we cannot be certain that the shells do not record only very local, within-strait sources, we view that to be unlikely on the basis of hydrographic tracer studies that show a predominantly Arctic Ocean origin of upper waters throughout the Strait (Alkire, 2010; K.K. Falkner et al., unpubl. data). Combined tracer and current studies measure fluxes of upper Arctic Ocean water through Nares Strait that exceed possible fluxes of local sources by orders of magnitude (Münchow et al., 2006).

If our bivalve collection sites are not affected by local sources of freshwater, then the oxygen isotopic composition of the shell should reflect the ambient δ^{18}O$_{water}$ and temperature of waters flowing through the Nares Strait. Currents through the CAA are multidirectional and complex (Fig. 1A, Rabe et al., 2010; K.K. Falkner et al., unpubl. data). They tap waters from both the Arctic Ocean and Baffin Bay, and superimposed on these are meteoric inputs, sea-ice melt and formation signals, glacial melt, and variable mixing processes. Hence, temperature and salinity vary regionally and temporally, particularly in the upper 100 to 200 m of the water column, where bivalves are most abundant (Alkire, 2010).

The imprint of variable δ^{18}O$_{water}$ on the δ^{18}O$_{carb}$ will be dampened with decreasing latitude in the strait, since upper Arctic waters are subject to considerable mixing as they transit the passages of the CAA (Melling et al., 1984; Alkire, 2010; K.K. Falkner et al., unpubl. data). Stations near the northern and western sides of Nares Strait (e.g., Bellot Island) are expected to show more variability in shell isotopic compositions with respect to δ^{18}O$_{water}$ because it is in these regions of the strait that the Arctic freshwater sources tend to be most pronounced (Alkire, 2010; Rabe et al., 2010; K.K. Falkner et al., unpubl. data). At the southern end (e.g., Littleton Island and Alexandra Fiord), Arctic freshwater signals are diluted with those in Baffin Bay. The expected pattern is indeed reflected in the measured isotopic compositions for the most recent year of shell accretion (Fig. 6).
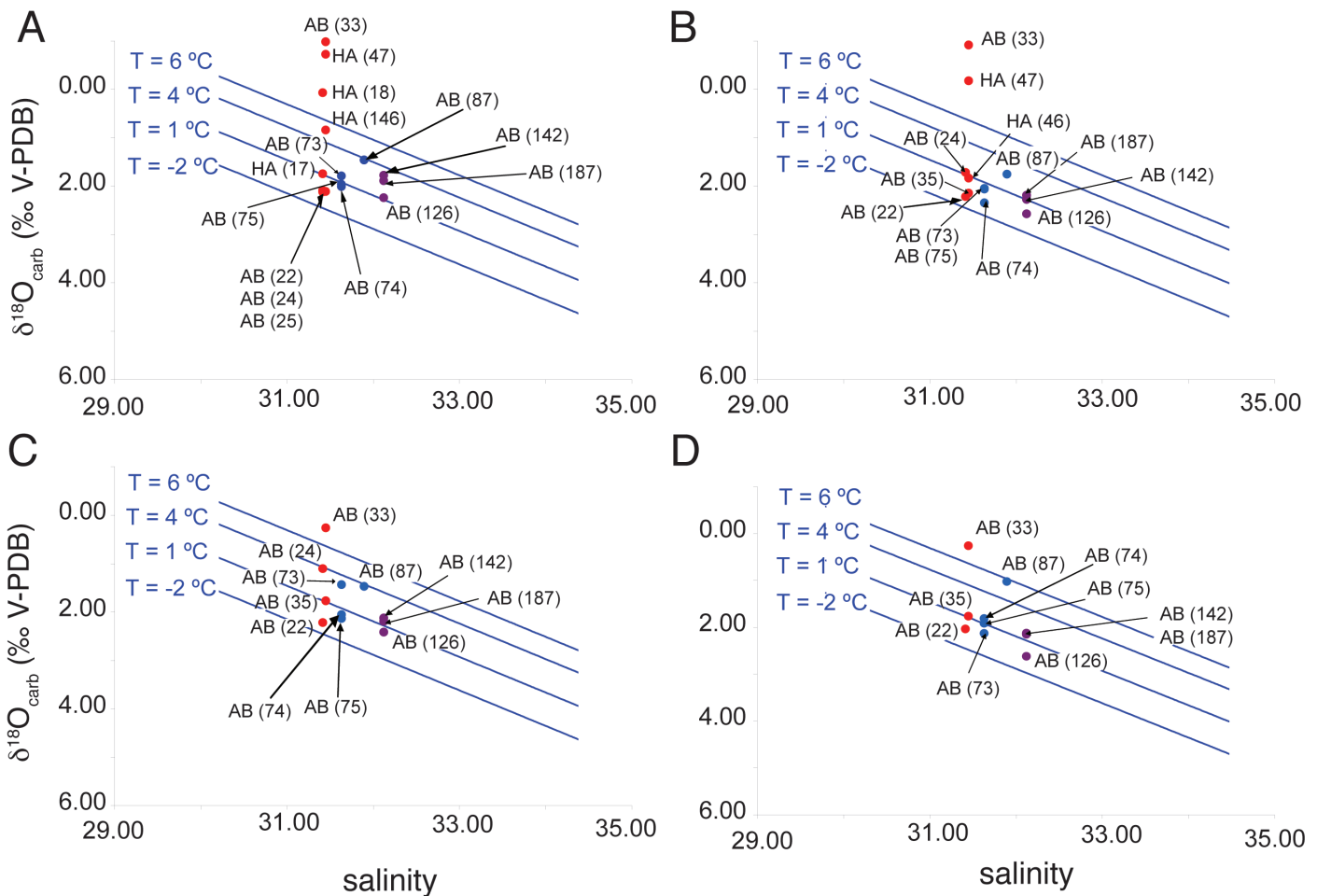
FIG. 7. Measured δ¹⁸O in shell sections corresponding to (A) 10 (± 5), (B) 20 (± 10), (C) 30 (± 10), and (D) 40 (± 10) years in specimens of *A. borealis* and *H. arctica* collected from Bellot Island (red dots), Offley Island (green dots), and Alexandra Fiord (purple dots). Measured values were compared to the expected isotopic composition of the aragonitic shells precipitated in equilibrium at discrete temperatures (solid lines). The numbers represent the identification numbers of the specimens used for drilling, and the two-letter abbreviations represent the bivalve species (see Table 3).

Note that the fractionation of the isotopes during sea-ice formation is only about +2.1‰ (Moore et al., 1983). Glacial runoff originating from Greenland would cause the freshening signal to increase southward. Thus we infer from our results that the increasingly fresh signal in recent time reflects rearranged circulation within the Arctic, which causes Nares Strait to receive proportionately more of the relatively fresh waters. The Beaufort Gyre appears to store and release pulses of freshwater to the Atlantic on decadal time scales (Proshutinsky et al., 2002; Dukhovskoy et al., 2006a, b). The timing of the freshening in our records is consistent with the so-called cyclonic Arctic Ocean Oscillation (AOO), a circulation pattern that corresponds to freshwater release from the Arctic (See Fig. 2 in Dukhovskoy et al., 2006b).

It is interesting that our most pronounced freshening occurred in the first cyclonic AOO year after a brief (4-year) anticyclonic regime that had followed a prolonged cyclonic regime. In that prolonged time-frame spanning most of the 1990s, the Arctic Oscillation index, which is an indication of the atmospheric state in the Northern Hemisphere, was highly positive and inversely correlated to the AOO. In the

preceding five decades, these indices had been positively correlated, which suggests that the Arctic system entered into a new state in the late 1980s. Our shell data suggest that this transition corresponds to a trend toward the fluxing of freshest waters through Nares Strait in the two most recent decades.

With oxygen isotopes alone, we cannot distinguish what portion of this freshening signal in our shells is due to decreased brine production and what portion to enhanced dilution by meteoric waters. There may be other chemical signatures in the shells that will allow these distinctions, but such work was beyond the scope of this exploratory study. There is evidence in historical hydrographic data that such a freshening effect has been accumulating downstream in the northwest area of Baffin Bay in recent decades (Zweng and Münchow, 2005).

CONCLUSIONS

Bivalve shells have proven to be useful recorders of the ambient hydrographic conditions in which these animals
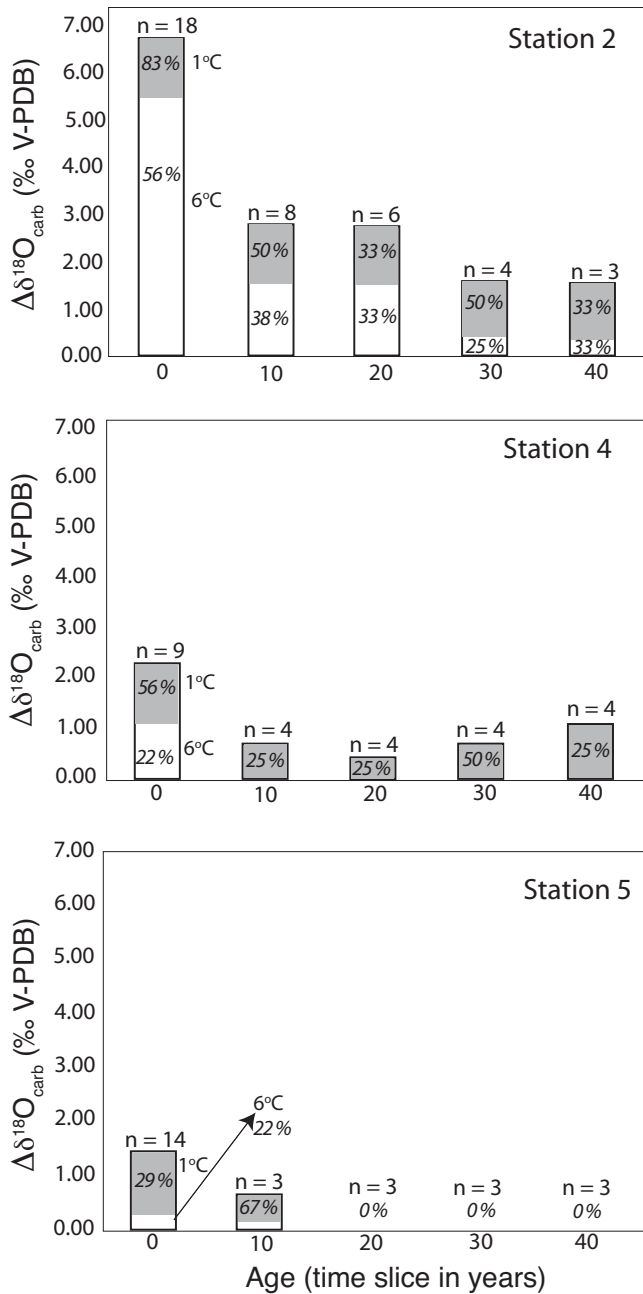
FIG. 8. Deviation from the expected oxygen isotopic shell values ($\Delta\delta^{18}O_{carb}$) using equation 4 and the $\delta^{18}O_{carb}$ measured in shell sections corresponding to the most recent year and 10, 20, 30, and 40 years of growth in specimens from the northernmost region of Nares Strait (Station 2), the approximate midpoint (Station 4), and the southernmost region (Station 5). Grey sections of bars represent the maximum range of deviation from expected values assuming an average temperature of 1°C, and white sections represent the range of deviation at 6°C, each indicating the fraction of the samples that were lighter in isotopic composition than expected (as percentage values shown in italics). N is the total number of shells that were drilled for the corresponding time slice.

grow. However, a robust interpretation of these proxies relies on understanding the features of the modern system, which has recently been characterized by Alkire (2010). Here we have analyzed the potential of bivalve shells to trace recent changes in the temperature and $\delta^{18}O_{water}$ of

shallow (< 30 m) waters of Nares Strait. Our data show that at the stations where bivalves were collected, the $\delta^{18}O_{water}$ is largely dominated by variations in salinity that are consistent with the general relationship observed in the greater Nares Strait region. This high correlation allowed us to use the $\delta^{18}O_{water}$ as a proxy for salinity.

Measured isotopic records for specimens of *H. arctica* and *A. borealis,* taken from shell sections corresponding to time slices at 10-year increments from the time of collection, indicate that the range of deviations from predicted isotopic values is most frequently largest in the latest 20 years, and decreases successively through the 30 and 40 year time slices. These results show a gradient in freshening trends from north to south consistent with proximity to sources in the north and along-strait mixing. Lighter-than-expected isotopic values are most prevalent at Station 2, which suggests that specimens at the northern end of Nares Strait began experiencing an increase in freshwater input as far back as the early 1980s, while other stations at the midpoint and southern end have experienced less pronounced freshening. These results are consistent both with current understanding of decadal trends affecting freshwater storage and circulation within the Arctic Ocean (Proshutinsky et al., 2002; Dukhovskoy et al., 2006a, b) and with historical hydrographic data that have indicated notable freshening in northwestern Baffin Bay over recent decades (Zweng and Münchow, 2005). Our study shows the considerable promise of bivalve records for helping to reconstruct time series of hydrographic conditions in the CAA. Future studies will benefit from enhanced temporal coverage and inclusion of additional chemical tracers in the shells.

REFERENCES

Aagaard, K., and Carmack, E.C. 1989. The role of sea ice and other fresh water in the Arctic Circulation. Journal of Geophysical Research 94(C10):14485–14498, doi:10.1029/JC 094iC10p14485.

Alkire, M.B. 2010. Differentiating freshwater contributions and their variability to the surface and halocline layers of the Arctic and subarctic seas. PhD thesis, Oregon State University, Corvallis, Oregon. 161 p. http://ir.library.oregonstate.edu/jspui/handle/1957/15188.

Alkire, M.B., Falkner, K.K., Rigor, I., Steele, M., and Morison, J. 2007. The return of Pacific waters to the upper layers of the central Arctic Ocean. Deep-Sea Research Part I 54:1509 – 1529, doi:10.1016/j.dsr.2007.06.004.

Amaro, T., Duineveld, G., Bergman, M., and Witbaard, R. 2003. Growth variations in the bivalve *Mya truncata*: A tool to trace changes in the Frisian Front macrofauna (southern North Sea)? Helgoland Marine Research 57:132 – 138.

Bauch, D., Schlosser, P., and Fairbanks, R.G. 1995. Freshwater balance and the sources of deep and bottom waters in the Arctic Ocean inferred from the distribution of $H_2^{18}O$. Progress in Oceanography 35:53 – 80, doi:10.1016/0079-6611(95)00005-2.

Bauch, D., Dmitrenko, I.A., Wegner, C., Hölemann, J., Kirillov, S.A., Timokhov, L.A., and Kassens, H. 2009. Exchange of Laptev Sea and Arctic Ocean halocline waters in response to atmospheric forcing. Journal of Geophysical Research 114, C05008, doi:10.1029/2008JC005062.

Böhm, F., Joachimski, M.M., Dullo, W.-C., Eisenhauer, A., Lehnert, H., Reitner, J., and Wörheide, G. 2000. Oxygen isotope fractionation in marine aragonite of coralline sponges. Geochimica et Cosmochimica Acta 64:1695 – 1703, doi:10.1016/S0016-7037(99)00408-1.

Cooper, L.W., McClelland, J.W., Holmes, R.M., Raymond, P.A., Gibson, J.J., Guay, C.K., and Peterson, B.J. 2008. Flow-weighted values of runoff tracers ($\delta^{18}O$, DOC, Ba, alkalinity) from the six largest Arctic rivers. Geophysical Research Letters 35, L18606, doi:10.1029/2008GL035007.

Degen, D. 2005. Sclerochronologische Untersuchungen an Muscheln aus Nord- und Ostsee. Diploma thesis, University of Frankfurt A.M., Germany. 73 p.

Dettman, D.L., Flessa, K.W., Roopnarine, P.D., Schöne, B.R., and Goodwin, D.H. 2004. The use of oxygen isotope variation in shells of estuarine mollusks as a quantitative record of seasonal and annual Colorado River discharge. Geochimica et Cosmochimica Acta 68:1253 – 1263.

Dickson, R.R., Osborn, T.J., Hurrell, J.W., Meincke, J., Blindheim, J., Adlandsvik, B., Vinje, T., Alekseev, G., and Maslowski, W. 2000. The Arctic Ocean response to the North Atlantic Oscillation. Journal of Climate 13:2671 – 2696.

Dukhovskoy, D., Johnson, M., and Proshutinsky, A. 2006a. Arctic decadal variability from an idealized atmosphere-ice-ocean model: 1. Model description, calibration, and validation. Journal of Geophysical Research 111, C06028, doi:10.1029/2004JC002821.

———. 2006b. Arctic decadal variability from an idealized atmosphere-ice-ocean model: 2. Simulation of decadal oscillations. Journal of Geophysical Research 111, C06029, doi:10.1029/2004JC002820, 2006.

Guay, C.K.H., McLaughlin, F.A., and Yamamoto-Kawai, M. 2009. Differentiating fluvial components of upper Canada Basin waters on the basis of measurements of dissolved barium combined with other physical and chemical tracers. Journal of Geophysical Research 114, C00A09, doi:10.1029/2008JC005099.

Israelson, C., Buchardt, B., Funder, S., and Hubberten, H.W. 1994. Oxygen and carbon isotope composition of Quaternary bivalve shells as a water mass indicator: Last interglacial and Holocene, East Greenland. Palaeogeography, Palaeoclimatology, Palaeoecology 111:119 – 134, doi:10.1016/0031-0182(94)90351-4.

Karcher, M.J., and Oberhuber, J.M. 2002. Pathways and modification of the upper and intermediate waters of the Arctic Ocean. Journal of Geophysical Research 107(C6), 3049, doi:10.1029/2000JC000530.

Khim, B.K. 2002. Stable isotope profiles of *Serripes groenlandicus* shells. I. Seasonal and interannual variations of Alaskan Coastal Water in the Bering and Chukchi seas. Geosciences Journal 6:257 – 267.

Khim, B.K., Krantz, D.E., and Brigham-Grette, J. 2001. Stable isotope profiles of last interglacial (Pelukian Transgression) molluscs and paleoclimate implications in the Bering Strait region. Quaternary Science Reviews 20:463 – 483, doi:10.1016/S0277-3791(00)00104-9.

Khim, B.K., Krantz, D.E., Cooper, L.W., and Grebmeier, J.M. 2003. Seasonal discharge of estuarine freshwater to the western Chukchi Sea shelf identified in stable isotope profiles of mollusk shells. Journal of Geophysical Research 108(C9), 3300, doi:10.1029/2003JC001816.

Kilada, R.W., Roddick, D., and Mombourquette, K. 2007. Age determination, validation, growth and minimum size of sexual maturity of the Greenland smoothcockle (*Serripes groenlandicus*, Bruguiere, 1789) in eastern Canada. Journal of Shellfish Research 26:443 – 450, doi:10.2983/0730-8000(2007)26[443:ADVGAM]2.0.CO;2.

Macdonald, R.W., Paton, D.W., Carmack, E.C., and Omstedt, A. 1995. The freshwater budget and under-ice spreading of Mackenzie River water in the Canadian Beaufort Sea based on salinity and $^{18}O/^{16}O$ measurements in water and ice. Journal of Geophysical Research 100(C1), 895 – 919, doi:10.1029/94JC02700.

Macdonald, R.W., McLaughlin, F.A., and Carmack, E.C. 2002. Fresh water and its sources during the SHEBA drift in the Canada Basin of the Arctic Ocean. Deep-Sea Research Part I 49:1769 – 1785, doi:10.1016/S0967-0637(02)00097-3.

McPhee, M.G., Proshutinsky, A., Morison, J.H., Steele, M., and Alkire, M.B. 2009. Rapid change in freshwater content of the Arctic Ocean. Geophysical Research Letters 6, L10602, doi:10.1029/2009GL037525.

Melling, H. 2000. Exchanges of freshwater through the shallow straits of the North American Arctic. In: Lewis, E.L., ed. The freshwater budget of the Arctic Ocean. Boston: Kluwer. 479 – 502.

Melling, H., Lake, R.A., Topham, D.R., and Fissel, D.B. 1984. Oceanic thermal structure in the western Canadian Arctic. Continental Shelf Research 3:233 – 258, doi:10.1016/0278-4343(84)90010-4.

Melling, H., Agnew, T.A., Falkner, K.K., Greenberg, D.A., Lee, C.M., Münchow, A., Petrie, B., Prinsenberg, S.J., Samelson, R.M., and Woodgate, R.A. 2008. Fresh-water fluxes via Pacific and Arctic outflows across the Canadian Polar Shelf. In: Dickson, R.R., Meincke, J., and Rhines, P., eds. Arctic-Subarctic Ocean fluxes: Defining the role of the northern seas in climate. Dordrecht, The Netherlands: Springer. 193 – 247.

Moore, R.M., Lowings, M.G., and Tan, F.C. 1983. Geochemical profiles in the Central Arctic Ocean: Their relation to freezing

and shallow circulation. Journal of Geophysical Research 88(C4), 2667–2674, doi:10.1029/JC088iC04p02667.

Müller-Lupp, T., and Bauch, H. 2005. Linkage of Arctic atmospheric circulation and Siberian shelf hydrography: A proxy validation using δ¹⁸O records of bivalve shells. Global and Planetary Change 48:175–186, doi:10.1016/j.gloplacha.2004.12.012.

Müller-Lupp, T., Erlenkeuser, H., and Bauch, H.A. 2003. Seasonal and interannual variability of Siberian River discharge in the Laptev Sea inferred from stable isotopes in modern bivalves. Boreas 32:292–303, doi:10.1080/03009480310001984.

Müller-Lupp, T., Bauch, H.A., and Erlenkeuser, H. 2004. Holocene hydrographical changes of the eastern Laptev Sea (Siberian Arctic) recorded in δ¹⁸O profiles of bivalve shells. Boreas 61:32–41, doi:10.1016/j.yqres.2003.09.003.

Münchow, A., Melling, H., and Falkner, K.K. 2006. An observational estimate of volume and freshwater flux leaving the Arctic Ocean through Nares Strait. Journal of Physical Oceanography 36:2025–2041.

Östlund, H.G., and Hut, G. 1984. Arctic Ocean water mass balance from isotope data. Journal of Geophysical Research 89(C4), 6373–6381, doi:10.1029/JC089iC04p06373.

Otterå, O.H., Drange, H., Bentsen, M., Kvamstø, N.G., and Jiang, D. 2003. The sensitivity of the present-day Atlantic meridional overturning circulation to freshwater forcing. Geophysical Research Letters 30(17), 1898, doi:10.1029/2003GL017578.

Peterson, B.J., Holmes, R.M., McClelland, J.W., Vörösmarty, C.J., Lammers, R.B., Shiklomanov, A.I., Shiklomanov, I.A., and Rahmstorf, S. 2002. Increasing river discharge to the Arctic Ocean. Science 298:2171–2173, doi:10.1126/science.1077445.

Proshutinsky, A., Bourke, R.H., and McLaughlin, F.A. 2002. The role of the Beaufort Gyre in Arctic climate variability: Seasonal to decadal climate scales. Geophysical Research Letters 29(23), 2100, doi:10.1029/2002GL015847.

Rabe, B., Münchow, A., Johnson, H.L., and Melling, H. 2010. Nares Strait hydrography and salinity field from a 3-year moored array. Journal of Geophysical Research 115, C07010, doi:10.1029/2009JC005966.

Renssen, H., Goosse, H., Fichefet, T., and Campin, J.-M. 2001. The 8.2 kyr BP event simulated by a global atmosphere-sea-ice-ocean model. Geophysical Research Letters 28(8):1567–1570, doi:10.1029/2000GL012602.

Rhoads, D.C., and Lutz, R.A. 1980. Growth patterns within the molluscan shell: An overview. In: Rhoads, D.C., and Lutz, R.A., eds. Skeletal growth of aquatic organisms. New York: Plenum Press. 203–248.

Saenko, O.A., Wiebe, E.C., and Weaver, A.J. 2003. North Atlantic response to the above-normal export of sea ice from the Arctic. Journal of Geopysical Research 108(C7), 3224, doi:10.1029/2001JC001166.

Schöne, B.R., Freyre Castro, A.D., Fiebig, J., Houk, S.D., Oschmann, W., and Kröncke, I. 2004. Sea surface water temperatures over the period 1884–1983 reconstructed from oxygen isotope ratios of a bivalve mollusk shell (Arctica islandica, southern North Sea). Palaeogeography, Palaeoclimatology, Palaeoecology 212:215–232, doi:10.1016/j.palaeo.2004.05.024.

Schöne, B.R., Fiebig, J., Pfeiffer, M., Gleβ, R., Hickson, J., Johnson, A.L.A., Dreyer, W., and Oschmann, W. 2005a. Climate records from a bivalved Methuselah (Arctica islandica, Mollusca; Iceland). Palaeogeography, Palaeoclimatology, Palaeoecology 228:130–148, doi:10.1016/j.palaeo.2005.03.049.

Schöne, B.R., Dunca, E., Fiebig, J., and Pfeiffer, M. 2005b. Mutvei's solution: An ideal agent for resolving microgrowth structures of biogenic carbonates. Palaeogeography, Palaeoclimatology, Palaeoecology 228:149–166, doi:10.1016/j.palaeo.2005.03.054.

Sejr, M.K., Jensen, K.T., and Rysgaard, S. 2002. Annual growth bands in the bivalve Hiatella arctica validated by a mark-recapture study in NE Greenland. Polar Biology 25:794–796, doi:10.1007/s00300-002-0413-8.

Selin, N.I. 2007. Shell form, growth and life span of Astarte arctica and A. borealis (Mollusca: Bivalvia) from the subtidal zone of northeastern Sakhalin. Russian Journal of Marine Biology 33:232–237, doi:10.1134/S1063074007040050.

Serreze, M.C., Walsh, J.E., Chapin, F.S., III, Osterkamp, T., Dyurgerov, M., Romanovsky, V., Oechel, W.C., Morison, J., Zhang, T., and Barry, R.G. 2000. Observational evidence of recent change in the northern high-latitude environment, Climatic Change 46:159–207.

Serreze, M.C., Maslanik, J.A., Scambos, T.A., Fetterer, F., Stroeve, J., Knowles, K., Fowler, C., Drobot, S., Barry, R.G., and Haran, T.M. 2003. A record minimum Arctic sea ice extent and area in 2002. Geophysical Research Letters 30(3), 1110, doi:10.1029/2002GL016406.

Serreze, M.C., Barrett, A.P., Slater, A.G., Woodgate, R.A., Aagaard, K., Lammers, R.B., Steele, M., Moritz, R., Meredith, M., and Lee, C.M. 2006. The large-scale freshwater cycle of the Arctic. Journal of Geophysical Research 111, C11010, doi:10.1029/2005JC003424.

Serreze, M.C., Barrett, A.P., and Slater, A.G. 2008. Variability and change in the atmospheric branch of the Arctic hydrologic cycle. In: Dickson, R.R., Meincke, J., and Rhines, P., eds. Arctic-Subarctic Ocean fluxes: Defining the role of the northern seas in climate. Dordrecht, The Netherlands: Springer. 343–362.

Simstich, J., Harms, I., Karcher, M.J., Erlenkeuser, H., Stanovoy, V., Kodina, L., Bauch, D., and Spielhagen, R.F. 2005. Recent freshening in the Kara Sea (Siberia) recorded by stable isotopes in Arctic bivalve shells. Journal of Geophysical Research 110, C08006, doi:10.1029/2004JC002722.

Steele, M.D., Thomas, D., and Rothrock, D. 1996. A simple model study of the Arctic Ocean freshwater balance, 1979–1985. Journal of Geophysical Research 20:20833–20848.

Steele, M., Morison, J., Ermold, W., Rigor, I., Ortmeyer, M., and Shimada, K. 2004. Circulation of summer Pacific halocline water in the Arctic Ocean. Journal of Geophysical Research 109, C02027, doi:10.1029/2003JC002009.

Stouffer, R.J., Yin, J., Gregory, J.M., Dixon, K.W., Spelman, M.J., Hurlin, W., Weaver, A.J., et al. 2006. Investigating the causes of the response of the thermohaline circulation to past and future climate changes. Journal of Climate 19:1365–1387.

Strain, P.M., and Tan, F.C. 1993. Seasonal evolution of oxygen isotope-salinity relationships in high-latitude surface waters. Journal of Geophysical Research 98(C8):14589–14598, doi:10.1029/93JC01182.

Tan, F.C., and Strain, P.M. 1980. The distribution of sea ice meltwater in the eastern Canadian Arctic. Journal of Geophysical Research 85:1925–1932.

———. 1996. Sea ice and oxygen isotopes in Foxe Basin, Hudson Bay, and Hudson Strait, Canada. Journal of Geophysical Research 101:20869–20876.

Walter, K.M., Zimov, S.A., Chanton, J.P., Verbyla, D., and Chapin, F.S., III. 2006. Methane bubbling from Siberian thaw lakes as a positive feedback to climate warming. Nature 443:71–75.

Wassenaar, L.I., Brand, U., and Terasmae, J. 1988. Isotopic and elemental geochemistry of marine invertebrates from the Late Quaternary Fort Langley Formation and Capilano Sediments, southwestern British Columbia, Canada. Chemical Geology, Isotope Geoscience Section 73:221–231.

Woodgate, R.A., and Aagaard, K. 2005. Revising the Bering Strait freshwater flux into the Arctic Ocean. Geophysical Research Letters 32, L02602, doi:10.1029/2004GL021747.

Yamamoto-Kawai, M., Tanaka, N., and Pivovarov, S. 2005. Freshwater and brine behaviors in the Arctic Ocean deduced from historical data of $\delta^{18}O$ and alkalinity (1929–2002 A.D.). Journal of Geophysical Research 110, C10003, doi:10.1029/2004JC002793.

Yamamoto-Kawai, M., McLaughlin, F.A., Carmack, E.C., Nishino, S., and Shimada, K. 2008. Freshwater budget of the Canada Basin, Arctic Ocean, from salinity, $\delta^{18}O$, and nutrients. Journal of Geophysical Research 113, C01007, doi:10.1029/2006JC003858.

Zima, D. 2007. Reconstructing salinity conditions in Nares Strait (Canadian Archipelago) from stable isotope profiles in bivalve shells. MS thesis, Oregon State University, Corvallis, Oregon. 117 p. http://ir.library.oregonstate.edu/jspui/handle/1957/3864.

Zweng, M.M., and Münchow, A. 2005. Warming and freshening of Baffin Bay, 1916–2003. Journal of Geophysical Research 111, C07016, doi:10.1029/2005JC003093.